

## On the Photophysics of Artificial Blue-Light Photoreceptors: An Ab Initio Study on a Flavin-Based Dye Dyad at the Level of Coupled-Cluster Response Theory

Keyarash Sadeghian and Martin Schütz\*

Contribution from the Institute of Physical and Theoretical Chemistry, University of Regensburg, Universitätsstrasse 31, D-93040 Regensburg, Germany

Received November 28, 2006; E-mail: martin.schuetz@chemie.uni-regensburg.de

**Abstract:** The photophysical behavior of a phenothiazine–phenyl–isoalloxazine dye dyad, a model system for blue-light photoreceptors functioning on the basis of photoinduced electron transfer, was investigated by employing a combination of time-dependent density functional and coupled-cluster response theory. A conical intersection between a “bright” locally excited and a “dark” charge-transfer state was found in the low-energy region of the corresponding potential energy surfaces. We propose that, for the solvated dyad, this conical intersection is responsible for the experimentally observed fast fluorescence quenching in that system.

### Introduction

Biological photoreceptors, sensing light from different regions of the visible spectrum, are important regulatory components for vital processes such as growth, development, color vision, circadian rhythms, and photomovement in bacteria, plants, and mammals.<sup>1</sup> Depending on the chemical structure of their photoactive chromophore and protein sequence alignment, they can be divided into six important families:<sup>2</sup> rhodopsins,<sup>3</sup> phytochromes,<sup>4</sup> xanthopsins,<sup>5</sup> phototropins,<sup>6–9</sup> cryptochromes,<sup>10</sup> and BLUF (blue light using flavin adenine dinucleotide) proteins.<sup>11</sup>

While the first three groups have different chromophores and undergo a cis–trans isomerization upon excitation, the last three have flavin as a light-sensitive component, each taking different primary steps in their photoactivated state.<sup>2</sup>

The photolyases<sup>12,13</sup> (also containing flavin) together with the last three families can be regarded as blue-light photoreceptors, which absorb in the blue (390–500 nm) and/or UV-A (320–390 nm) regions of the spectrum.<sup>14</sup> Common features of cryptochrome and photolyase are the initial processes in their

photochemistry. In both cases, a light-harvesting antenna, methylenyltetrahydrofolate (MTHF) for cryptochrome and pterin for photolyase, is used for an efficient photon absorption followed by an energy transfer of the Förster type to the catalytic chromophore, that is, the flavin. The photoinduced electron transfer (PET) to the signaling partner is then triggered at the excited state of the flavin.<sup>15,16</sup>

With the aim of mimicking the function of a blue-light photoreceptor of cryptochrome type, a molecular arrangement of covalently linked pyrene, isoalloxazine, and phenothiazine dye units was synthesized by Daub and co-workers.<sup>17</sup> Pyrene acts as an antenna, isoalloxazine (flavin) as an electron acceptor/redox mediator, and phenothiazine as the electron donor of the system (see compound 1 in ref 17). The role of phenothiazine as an electron donor has been studied before.<sup>18</sup> Flavin-related dyes have been under investigation in the context of redox-enzyme mimetic<sup>19,20</sup> or modeling natural photosynthesis.<sup>21</sup> In general, similar types of molecular systems have been looked at over the years, with the aim of improving our understanding of the electron-transfer processes as well as developing molecular devices such as optical switches<sup>22–26</sup> or components for

- (1) Christie, J. M.; Briggs, W. R. *J. Biol. Chem.* **2001**, *276*, 11457.
- (2) van der Horst, M. A.; Hellingwerf, K. J. *Acc. Chem. Res.* **2004**, *37*, 13.
- (3) Hoff, W. D.; Jung, K. H.; Spudich, J. L. *Annu. Rev. Biophys. Biomol. Struct.* **1997**, *26*, 223.
- (4) Quail, P. H. *Philos. Trans. R. Soc., Ser. London B* **1998**, *353*, 1399.
- (5) Kort, R.; Hoff, W. D.; van West, M.; Kroon, A. R.; Hoffer, S. M.; Vlieg, K. H.; Crielgaard, W.; van Beeumen, J. J.; Hellingwerf, K. J. *EMBO J.* **1996**, *15*, 3209.
- (6) Huala, E.; Oeller, P. W.; Liscum, E.; Han, I. S.; Larsen, E.; Briggs, W. R. *Science* **1997**, *278*, 2120.
- (7) Swartz, T. E.; Corchnoy, S. B.; Christie, J. M.; Lewis, J. W.; Szundi, I.; Briggs, W. R.; Bogomolni, R. A. *J. Biol. Chem.* **2001**, *276*, 36493.
- (8) Crosson, S.; Moffat, K. *Proc. Natl. Acad. Sci. U.S.A.* **2001**, *98*, 2995.
- (9) Holzer, W.; Penzkofer, A.; Fuhrmann, M.; Hegemann, P. *Photochem. Photobiol.* **2002**, *75*, 479.
- (10) Ahmad, M.; Cashmore, A. R. *Nature* **1993**, *366*, 162.
- (11) Gomelsky, M.; Klug, G. *Trends Biochem. Sci.* **2002**, *27*, 497.
- (12) Heelis, P. F.; Hartman, R. F.; Rose, S. D. *Chem. Soc. Rev.* **1995**, *24*, 289.
- (13) Carell, T.; Epple, R. *Eur. J. Org. Chem.* **1998**, 1245.
- (14) Briggs, W. R.; Huala, E. *Annu. Rev. Cell. Dev. Biol.* **1999**, *15*, 33.

- (15) Cashmore, A.; Jarillo, J. A.; Wu, Y.-J.; Lium, D. *Science* **1999**, *284*, 760.
- (16) Lin, C. *Trends Plant Sci.* **2000**, *5*, 337.
- (17) Shen, Z.; Strauss, J.; Daub, J. *Chem. Commun.* **2002**, 460.
- (18) Knorr, A.; Daub, J. *Angew. Chem., Int. Ed. Engl.* **1997**, *36*, 2817.
- (19) Takeda, J.; Ota, S.; Hirobe, M. *J. Am. Chem. Soc.* **1987**, *109*, 7677.
- (20) König, B.; Pelka, M.; Zieg, H.; Ritter, T.; Bouas-Laurent, H.; Bonneau, R.; Desvergne, J. P. *J. Am. Chem. Soc.* **1999**, *121*, 1681.
- (21) Hermann, D. T.; Schindler, A. C.; Polborn, K.; Gompper, R.; Stark, S.; Parusel, A. B. J.; Grabner, G.; Köhler, G. *Chem.—Eur. J.* **1999**, *5*, 3208.
- (22) Niemi, A.; Rotello, V. M. *Acc. Chem. Res.* **1999**, *32*, 44.
- (23) Trieflinger, C.; Röhr, H.; Rurack, K.; Daub, J. *Angew. Chem., Int. Ed.* **2005**, *44*, 2288.
- (24) Debreczeny, M. P.; Svec, W. A.; Marsh, E. M.; Wasielewski, M. R. *J. Am. Chem. Soc.* **1996**, *118*, 8174.
- (25) Debreczeny, M. P.; Svec, W. A.; Wasielewski, M. R. *Science* **1996**, *274*, 584.
- (26) Lukas, S.; Miller, E. E.; Wasielewski, M. R. *J. Phys. Chem. B* **2000**, *104*, 931.

organic emitting diodes (OLEDs).<sup>18,27</sup>

In the present work, we are interested in the phenothiazine–phenyl–isoalloxazine dyad which is the donor–acceptor part of the proposed arrangement (see compound 3 in ref 17). Spectroelectrochemistry measurements carried out on this dyad<sup>28</sup> show the formation of a radical cation with the oxidation localized at the phenothiazine and a radical anion and the reduction at the isoalloxazine subunit. Fluorescence measurements on this dyad show an extremely low fluorescence quantum yield ( $\Phi_F = 0.0005$ ) upon excitation in the long wavelength band (463 nm = 2.68 eV), an indication for an efficient fluorescence quenching of the isoalloxazine moiety. In the time-resolved fluorescence measurements published by Schneider et al.,<sup>28</sup> the short-living component could not be resolved, and only a long-living component of 6 ns was reported. More recent time-resolved measurements<sup>29</sup> determine a biexponential decay with a fast component of 600 fs and a slow component of 4.5 ns. A semiempirical AM1 study on these dyads and triads has been reported before by Clark and co-workers.<sup>28,30,31</sup> Furthermore, the excited states of flavin and related molecules (uracil, isolumazine, and lumiflavin) have been studied by Neiss et al.,<sup>32,33</sup> whereas for phenothiazine and its derivatives, there are, to our best knowledge, only semiempirical, DFT, and HF calculations of the ground state available in the literature.<sup>34–36</sup>

In this contribution, we present the results of an ab initio study on the excited states of the phenothiazine–phenyl–isoalloxazine dyad, which was slightly simplified for our calculations (vide infra). We have employed a combination of time-dependent density functional theory (TD-DFT)<sup>37–40</sup> on the one hand to optimize excited-state geometries and coupled-cluster (CC2) linear response theory<sup>41–44</sup> on the other hand to obtain reasonably accurate excitation energies. The underlying assumption is that equilibrium structures are much less effected than excitation energies by the notorious self-interaction problem of DFT for charge-transfer (CT) states. Our calculations reveal a conical intersection between a locally excited (LE) and a CT state, which we assume to be the origin of the short lifetime and fluorescence quenching observed in the experiments mentioned above.

The fact that conical intersections<sup>45–47</sup> are important for the photochemistry of organic molecules is nothing new and has been investigated over the years in different systems in combination with various ab initio methods.<sup>48–54</sup> Conical intersections of excited states with the ground state provide highly efficient deactivation channel/funnels for the radiationless decay of these excited states. Nature, thus, exploits conical intersections of this type to stabilize vital biomolecules such as DNA against photodegradation.<sup>55</sup> Theoretical and experimental investigations carried out on 2-aminopyridine dimers<sup>56</sup> mimicking Watson–Crick base pairs in DNA show a proton-transfer step connecting the locally excited and charge-transfer states with the ground state through two conical intersections.<sup>56,57</sup> The short lifetime of the excited state ( $65 \pm 10$  ps) observed<sup>56</sup> in this system reveals the importance of such fast radiationless decay mechanisms which protect the living organism from the UV part of the sunlight. Similar situations are also encountered in studies on guanine–cytosine base pairs,<sup>58,59</sup> 9H-adenine isomer,<sup>60</sup> and salicylic acid.<sup>61</sup>

Furthermore, conical intersections between two excited states may determine the photophysical behavior of many molecules. One frequently discussed example of this type is 4-(dimethylamino)benzonitrile (DMABN), which has been studied extensively both experimentally and theoretically (cf. ref 62 and references therein). A CI between two excited states of different character, an LE and a CT state, is responsible for the dual fluorescence of this molecule. A similar situation is encountered in the present study for the phenothiazine–phenyl–isoalloxazine dyad, though no fluorescence out of the CT state is observed here due to the low transition strength of that state.

## Computational Details

The molecule investigated in the present study is depicted in Figure 1 and comprises 53 atoms (172 valence electrons), 36 of which are second-row elements. Considering, furthermore, that 153 degrees of freedom are to be relaxed in the geometry optimizations of the ground and excited states, the system is quite large compared to other molecules, which to our knowledge, have been studied previously at the same level of theory. Hence, a point to bare in mind at this stage is the limited feasibility of a detailed and accurate study on the excited-

(27) Gong, X.; Ng, P. K.; Chan, W. K. *Adv. Mater.* **1998**, *10*, 1337.

(28) Shen, Z.; Procházka, R.; Daub, J.; Fritz, N.; Acar, N.; Schneider, S. *Phys. Chem. Chem. Phys.* **2003**, *5*, 3257.

(29) Shirdel, J.; Penzkofer, A.; Procházka, R.; Daub, J. Manuscript in preparation.

(30) Acar, N.; Kurzawa, J.; Fritz, N.; Stockmann, A.; Roman, C.; Schneider, S.; Clark, T. *J. Phys. Chem. A* **2003**, *107*, 9530.

(31) Stockmann, A.; Kurzawa, J.; Fritz, N.; Acar, N.; Schneider, S.; Daub, J.; Engl, R.; Clark, T. *J. Phys. Chem. A* **2002**, *106*, 7958.

(32) Neiss, C.; Saalfrank, P. *Photochem. Photobiol.* **2003**, *1*, 77.

(33) Neiss, C.; Saalfrank, P.; Parac, M.; Grimme, S. *J. Phys. Chem. A* **2003**, *107*, 140.

(34) Bolboaca, M.; Iliescu, T.; Paiz, C.; Irimie, F. D.; Kiefer, W. *J. Phys. Chem. A* **2003**, *107*, 1811.

(35) Pan, D.; Phillips, D. L. *J. Phys. Chem. A* **1999**, *103*, 4737.

(36) Palafox, M. A.; Gil, M.; Núñez, J. L.; Tardajos, G. *Int. J. Quantum Chem.* **2002**, *89*, 147.

(37) Casida, M. E. In *Recent Advances in Density Functional Methods, Part I*; Chong, D., Ed.; World Scientific: Singapore, 1995.

(38) Gross, E. U. K.; Dobson, J. F.; Petersilka, M. In *Density Functional Theory II*; Nalewajski, R., Ed.; Springer: Heidelberg, Germany, 1996.

(39) Furche, F. *J. Chem. Phys.* **2001**, *114*, 5982.

(40) Furche, F.; Ahlrichs, R. *J. Chem. Phys.* **2002**, *117*, 7433.

(41) Koch, H.; Jørgensen, P. *J. Chem. Phys.* **1990**, *93*, 3333.

(42) Koch, H.; Jensen, H. J. A.; Jørgensen, P.; Helgaker, T. *J. Chem. Phys.* **1990**, *93*, 3345.

(43) Christiansen, O.; Jørgensen, P.; Hättig, C. *Int. J. Quantum Chem.* **1998**, *68*, 1.

(44) Christiansen, O.; Koch, H.; Jørgensen, P. *Chem. Phys. Lett.* **1995**, *243*, 409.

(45) Michl, J.; Klessinger, M. In *Excited States and Photochemistry of Organic Molecules*; VCH: New York, 1995.

(46) Klessinger, M. *Angew. Chem., Int. Ed. Engl.* **1995**, *34*, 549.

(47) Migani, A.; Olivucci, M. In *Conical Intersections: Electronic Structure, Dynamics and Spectroscopy*; Domcke, W.; Yarkony, D.; Köppel, H., Eds.; World Scientific: Singapore, 2004.

(48) Bernardi, F.; Olivucci, M.; Robb, M. A. *Chem. Soc. Rev.* **1996**, *25*, 321.

(49) Boggio-Pasqua, M.; Bearpark, M.; Hunt, P. A.; Robb, M. A. *J. Am. Chem. Soc.* **2002**, *124*, 1456.

(50) Bearpark, M.; Bernardi, F.; Clifford, S.; Olivucci, M.; Robb, M. A.; Smith, B. R.; Vreven, T. *J. Am. Chem. Soc.* **1996**, *118*, 169.

(51) Sanchez-Galvez, A.; Hunt, P.; Robb, M. A.; Olivucci, M.; Vreven, T.; Schlegel, H. B. *J. Am. Chem. Soc.* **2000**, *122*, 2911.

(52) Coto, P. B.; Sinicropi, A.; De Vico, L.; Ferré, N.; Olivucci, M. *Mol. Phys.* **2006**, *104*, 655.

(53) Ruiz, D. S.; Cembran, A.; Garavelli, M.; Olivucci, M.; Fuss, W. *Photochem. Photobiol.* **2002**, *76*, 622.

(54) Zilberg, S.; Haas, Y. *J. Phys. Chem. A* **2002**, *106*, 1.

(55) Abo-Riziq, A.; Grace, L.; Nir, E.; Kabelac, M.; Hobza, P.; de Vries, M. *Proc. Natl. Acad. Sci. U.S.A.* **2005**, *102*, 20 and references therein.

(56) Schultz, T.; Samoylova, E.; Radloff, W.; Hertel, I. V.; Sobolewski, A. L.; Domcke, W. *Science* **2004**, *306*, 1765.

(57) Sobolewski, A.; Domcke, W. *Chem. Phys.* **2003**, *294*, 73.

(58) Sobolewski, A. L.; Domcke, W. *Phys. Chem. Chem. Phys.* **2004**, *6*, 2763.

(59) Sobolewski, A.; Domcke, W.; Hättig, C. *Proc. Natl. Acad. Sci. U.S.A.* **2005**, *102*, 17903.

(60) Perun, S.; Sobolewski, A. L.; Domcke, W. *J. Am. Chem. Soc.* **2005**, *127*, 6257.

(61) Sobolewski, A. L.; Domcke, W. *Phys. Chem. Chem. Phys.* **2006**, *8*, 3410.

(62) Gomez, I.; Reguero, M.; Boggio-Pasqua, M.; Robb, M. A. *J. Am. Chem. Soc.* **2005**, *127*, 7119.



**Table 1.** TD-DFT and CC2 Vertical Excitation Energies (in eV, Ordered According to the CC2 Values) Calculated at the DFT-Optimized Ground-State Equilibrium Geometry<sup>a</sup>

character	TD-DFT/BP			TD-DFT/B3-LYP			CC2		
	E(eV)	<i>f</i>	$ \bar{\mu}(\text{ex}) $	E(eV)	<i>f</i>	$ \bar{\mu}(\text{ex}) $	E(eV)	<i>f</i>	$ \bar{\mu}(\text{ex}) (\mu_x, \mu_y, \mu_z)$
S <sub>0</sub>			9.136			8.973			8.366 (6.81, 4.63, -1.35)
LE $\pi \rightarrow \pi^*$	2.683	0.079	11.669	3.029	0.189	13.018	3.233	0.242	11.263 (7.43, 8.30, -1.62)
LE $\pi \rightarrow \pi^*$	2.457	0.001	16.185	3.154	0.000	15.126	3.416	0.004	15.286 (5.16, 14.25, -1.96)
CT $\pi \rightarrow \pi^*$	0.953	0.002	45.466	1.834	0.002	46.034	3.530	0.010	32.708 (6.17, 32.05, -2.09)
PCT $\pi \rightarrow \pi^*$	2.569	0.131	27.265	3.130	0.154	15.240	3.679	0.202	11.595 (5.50, 10.19, -0.54)
LE $n \rightarrow \pi^*$	2.037	0.001	24.233	3.001	0.001	4.778	3.701	0.020	10.082 (0.48, 9.86, -2.06)

<sup>a</sup> Ground- and excited-state dipole moments (in debye), as well as the related oscillator strengths (*f*) in length representation, are also given.

The computational cost of the CC2 linear response method based on DF scales as  $\mathcal{O}(N^5)$  with the molecular size  $N$  in a canonical implementation. This makes calculations on molecules of this size or even bigger very costly, in particular, for properties of excited states. Therefore, geometry optimizations at the level of CC2 are presently restricted to molecules of considerably smaller size.<sup>61,80</sup>

Presently, a new CC2 linear response method based on localized orbitals with a more favorable scaling of the computational cost is under development in our group. This local CC2 (LCC2) response method,<sup>81,82</sup> implemented in the present development version of the MOLPRO package,<sup>83</sup> has been used to study the effect of the solvent on the vertical excitation energies of the LE and CT states. For these local calculations, the cc-pVDZ basis<sup>84</sup> together with the related fitting basis<sup>85</sup> was used. The pair list for the ground state (GS) amplitudes included all pairs with interorbital distances not exceeding 10 bohr, while the GS domains were determined according to a Boughton–Pulay<sup>91</sup> criterion of 0.985. Pair lists and domains of the individual excited states, such as the related amplitudes response, were determined based on an analysis of an initial CIS (configuration interaction singles) wave function, as described in detail in ref 81. For this purpose, the criterion for “important orbital” selection was set to  $\kappa_c = 0.995$ , while the related pair list included all pairs of important orbitals and pairs of all other orbitals up to an interorbital distance of 10 bohr. This is a rather conservative specification of the pair list, as shown in ref 81.

## Results and Discussion

**At the Ground-State Geometry.** The CC2 linear response calculations at the DFT-optimized ground-state equilibrium geometry reveal that the first excited state S<sub>1</sub> is of the  $\pi \rightarrow \pi^*$  type (HOMO-2  $\rightarrow$  LUMO) and primarily localized on the isoalloxazine subunit (plots of the relevant orbitals are given in Figure 2). It has the highest oscillator strength<sup>86,87</sup> ( $f = 0.242$ ) within the five lowest calculated excited states of the dyad (cf. Table 1).

In the following, we will synonymously use the notation LE state (locally excited state) for this S<sub>1</sub> state. The S<sub>2</sub> state, again, is primarily localized on the isoalloxazine subunit; however it has an almost negligible oscillator strength. The S<sub>3</sub> state is the charge-transfer state, dominated by the HOMO  $\rightarrow$  LUMO  $\pi \rightarrow \pi^*$  orbital substitution with negative charge transferred from phenothiazine to isoalloxazine. It has, consequently, an

appreciably higher dipole moment than that of the other states, but its oscillator strength is, again, very small ( $f = 0.01$ ). Since the minimum-energy geometry of the CT state surface is markedly different from the ground-state equilibrium geometry (vide infra), the related Franck–Condon factors are presumed to be small as well. The next state has some CT character too, involving the phenothiazine and the bridging phenyl group (dominated by the HOMO  $\rightarrow$  LUMO+1 orbital substitution, see Figure 2), although its dipole moment calculated at the DFT/B3-LYP level is not significantly larger than that of the LE state. We will denote this state in the following as the PCT (partial charge-transfer) state. The fifth state, finally, is again localized on the isoalloxazine subunit and has  $n \rightarrow \pi^*$  character.

The formation of the charge-separated species (D<sup>+</sup>–A<sup>−</sup>) observed in the experiments<sup>28</sup> leads us to the hypothesis that the dark CT state (with low oscillator strength) is responsible for the fluorescence quenching of the LE state. Since the CT state lies energetically above the LE state at the ground-state equilibrium geometry and below the LE state at the CT minimum-energy geometry, it can be anticipated that a conical intersection between these two states exists.

In contrast to the CC2 calculation, TD-DFT provides an entirely different physical picture. Here, the dark CT state lies far below the bright LE state (by 1.2–1.7 eV). Depending on the functional, the excitation energy for the CT state is 2.5 (BP) and 1.6 eV (B3-LYP) smaller than the corresponding CC2 value, clear indications of large self-interaction errors also for the B3-LYP functional. For the PCT state, the deviations between DFT and CC2 are a bit smaller, −1.11 and −0.35 eV for the BP and the B3-LYP functionals, respectively, reflecting the shorter distance between donor and acceptor. The TD-DFT and CC2 dipole moments are quite similar for the locally excited states but again differ considerably for the CT state, a further sign of a severe self-interaction problem in TD-DFT.

**At the CT Minimum-Energy Geometry.** Since the CT state is energetically well-separated from all other states at the level of TD-DFT, it was readily possible to determine its minimum-energy geometry by relaxing all degrees of freedom. On going from the ground state to the CT minimum-energy geometry, significant structural changes do occur, as shown in Table 3; the dihedral angles  $\theta_1$  and  $\theta_2$  (cf. Figure 1) within the phenothiazine subunit change by  $\Delta\theta_1 = -14.9^\circ$  and  $\Delta\theta_2 = -27.4^\circ$ , respectively, with the phenothiazine becoming virtually planar in the CT state, while torsional angles between the individual subunits alter by  $\Delta\alpha = -14.9^\circ$  (phenyl–phenothiazine) and  $\Delta\beta = -8.6^\circ$  (phenyl–isoalloxazine).

The related changes in the bond distances are compiled in Table 4. We observe elongations of all C–N and C=O bonds and contractions of all C–C bonds of the isoalloxazine, shown

(80) Köhn, A.; Hättig, C. *J. Am. Chem. Soc.* **2004**, *126*, 7399.

(81) Kats, D.; Korona, T.; Schütz, M. *J. Chem. Phys.* **2006**, *125*, 104106.

(82) Kats, D.; Korona, T.; Schütz, M. Manuscript in preparation.

(83) Werner, H.-J.; et al. *MOLPRO*, version 2006.2, a package of ab initio programs; 2006 (<http://www.molpro.net>).

(84) Dunning, T. H., Jr.; Hay, P. J. In *Methods of Electronic Structure Theory*; Schaefer, H. F., III, Ed.; Plenum Press: New York, 1977; Vol. 2.

(85) Weigend, F.; Köhn, A.; Hättig, C. *J. Chem. Phys.* **2002**, *116*, 3175.

(86) The oscillator strength between states *m* and *n* is defined as  $f_{mn} \propto \bar{\nu}_{\text{max}} \cdot |\mu_{mn}|^2$ , with  $\mu_{mn} = \langle \Psi_m | \mu | \Psi_n \rangle$  denoting the corresponding transition dipole moment and  $\bar{\nu}_{\text{max}}$  the energy of the peak of the absorption band in wave numbers.<sup>87</sup>

(87) Gilbert, A.; Baggott, J. *Essentials of Molecular Photochemistry*; Blackwell Scientific Publications: Oxford, U.K., 1991.

**Table 2.** TD-DFT and CC2 Vertical Excitation Energies (in eV, Ordered According to the CC2 Values) Calculated at the DFT-Optimized CT-State Minimum-Energy Geometry<sup>a</sup>

character	TD-DFT/BP			TD-DFT/B3-LYP			CC2			
	E(eV)	<i>f</i>	$ \bar{\mu}(\text{ex}) $	E(eV)	<i>f</i>	$ \bar{\mu}(\text{ex}) $	E(eV)	<i>f</i>	$ \bar{\mu}(\text{ex}) (\mu_x, \mu_y, \mu_z)$	
CT $\pi \rightarrow \pi^*$	0.671	0.001	42.892	1.365	0.000	45.715	2.956	0.000	46.844 (22.87, 126.98, -2.26)	
LE $\pi \rightarrow \pi^*$	2.729	0.074	10.507	3.000	0.146	11.865	3.114	0.190	11.170 (8.35, 7.40, -0.44)	
LE $\pi \rightarrow \pi^*$	2.493	0.002	20.854	2.915	0.000	9.192	3.421	0.001	8.863 (2.13, 8.50, -1.34)	
LE $n \rightarrow \pi^*$	1.986	0.001	7.051	2.817	0.004	31.645	3.487	0.001	6.043 (2.37, 5.43, -1.20)	
PCT $\pi \rightarrow \pi^*$	2.540	0.116	17.379	3.071	0.079	12.975	3.518	0.102	10.766 (7.18, 8.02, 0.29)	

<sup>a</sup> The excited-state dipole moments (in debye), as well as the related oscillator strengths (*f*) in length representation, are also given.

in Table 4. The C21–N29 double bond lengthening by nearly 9 pm appears to be, by far, the most energetic bond (this bond is also important for the Cysteinyflavin addition reactions, as shown in the model study by Neiss et al.<sup>32</sup>), followed by the two C21–C27 and C21–C22 single bonds, which both become shorter by 4.1 pm. The contractions of the C4–S8 and the C3–N31 single bonds in phenothiazine lead to the planarity of this subsystem, which is reached at the CT-min structure. All of these bond contractions shown in Table 4 can already qualitatively be predicted based on the simple orbital picture given in Figure 2.

It is evident by comparing Tables 1 and 2 that the energetic order of the LE and CT states (computed at the level of CC2 linear response theory) is interchanged with the CT state now lying below the LE state. This is indicative of the presence of a conical intersection (CI) between these two states. TD-DFT, on the other hand, does not show anything alike, drawing an entirely different picture of the photophysics of the system. Furthermore, in contrast to CC2, there is no increase in the dipole moment of the CT state at the TD-DFT level, as can be seen in Tables 1 and 2.

**At the Conical Intersection Structure.** In order to map the low-energy region of the conical intersection seam between the LE and CT states, we choose to explore the CT surface, which is well-separated from all other states at the TD-DFT level and, therefore, much easier to treat when it comes to geometry optimizations. Of course, a more natural choice would have been to follow the LE state; however, geometry optimizations of that state turned out to be difficult due to mixing with other states. Note that the strongly absorbing LE state at the TD-DFT level is not the  $S_1$  or  $S_2$  but rather the  $S_8$  or  $S_5$  state, depending on the functional in use, which, in addition, is surrounded by weak  $\pi\pi^*$  artifact states of TD-DFT, the latter occurring at much higher energy at the CC2 level. As a consequence, TD-DFT geometry optimizations of the LE state are hampered by root flipping, which leads to severe convergence problems.

A 3D subspace,  $\mathcal{V}$ , within the space of all nuclear degrees of freedom was then defined, spanned by three fixed linear combinations of bond distances (stretch), bond angles (bend), and dihedral angles (torsion) (for technical reasons, mixed linear combinations between bond angles and, e.g., dihedral angles could not be used). To specify these three fixed linear combinations, the TD-DFT gradient of the CT state surface at the GS minimum-energy structure was projected onto the subspaces of the bond distances, the bond angles, and the dihedral angles. The resulting three projections of the gradient so obtained specify the basis of our subspace  $\mathcal{V}$ ; the  $3N - 9$  remaining coordinates are determined such that they form the orthogonal complement to  $\mathcal{V}$ . About 100 geometries interpolating between the ground-state equilibrium and the CT minimum-energy

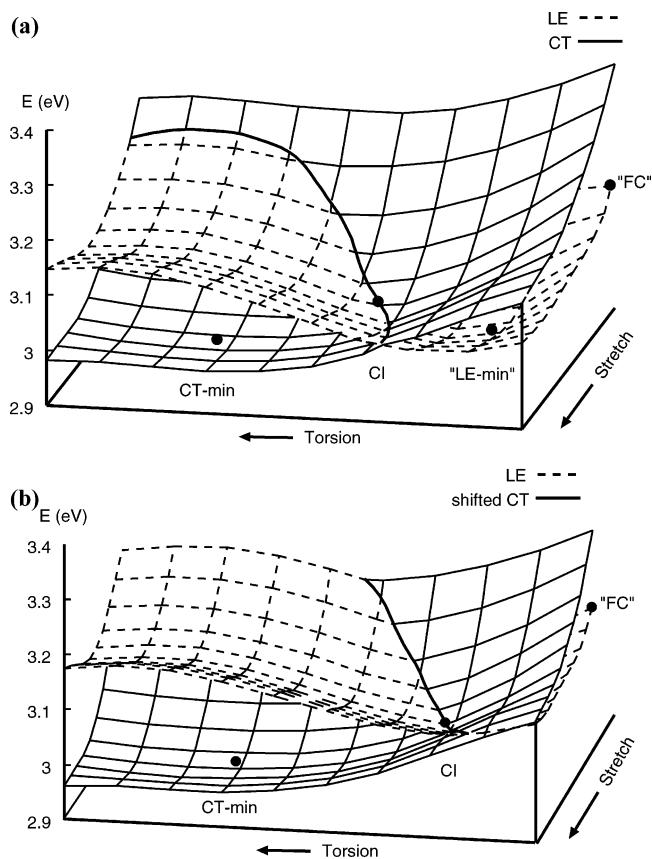


**Figure 3.** LE and CT surfaces within the 2D subspace of  $\mathcal{V}$  containing the CT-min and CI structures (bend angle is set to  $4^\circ$ ). The ground-state minimum geometry has a bend angle of  $0^\circ$  and does not lie within this 2D subspace; hence, the projection of the Franck–Condon point onto this subspace, indicated by “FC”, is given instead (a). The effect of the relative stabilization of the CT state in the acetonitrile solvent cluster (by 0.068 eV, vide infra) on the location of the CI seam is demonstrated in (b) by simply shifting the CT surface relative to the LE surface to lower energies by this amount (cf. Table 5).

structure within  $\mathcal{V}$  were then generated by relaxing all coordinates in the orthogonal complement to  $\mathcal{V}$ . Note that both the ground-state equilibrium structure (by construction) as well as the CT minimum-energy structure lie within  $\mathcal{V}$  (since the coordinates of the orthogonal complement are relaxed on the CT surface). For all of these points, CC2 excitation energies of the CT and LE state were then computed, generating two surfaces (depicted in Figure 3a), from which the conical intersection seam and its lowest energy point were deduced. In the following, we shall refer to the geometry of the minimum of the CI seam as the CI geometry. It is evident from Table 3 that the phenothiazine at the CI geometry still is nonplanar. (The  $\theta$  angles are well above zero!) The other two twist angles joining the subunits lie in between their values at the GS and the CT

**Table 3.** Dihedral Angles (Torsions) between Phenothiazine and Phenyl ( $\alpha$ ), Isoalloxazine and Phenyl ( $\beta$ ), and Those Responsible for the (Non)planarity of Phenothiazine ( $\theta_1$  and  $\theta_2$ )<sup>a</sup>

torsion	S <sub>0</sub>	LE ( $\Delta$ )	CI ( $\Delta$ )	CT ( $\Delta$ )
$\alpha$	-33.4	-27.6 (5.8)	-38.8(-5.4)	-48.3 (-14.9)
$\beta$	95.2	94.1 (-1.1)	90.0(-5.2)	86.6 (-8.6)
$\theta_1$	28.7	34.0 (5.3)	21.2 (-7.5)	-1.2 (-29.9)
$\theta_2$	26.8	27.5 (0.7)	16.9 (-9.9)	-0.6 (-27.4)

<sup>a</sup> For definition of these angles, see Figure 1.

**Table 4.** Bond Distances which Differ from Their Ground-State Geometry ( $\Delta$ ) by More Than 3 pm at Any of the Three CT-min, LE-min, or CI Geometries<sup>a</sup>

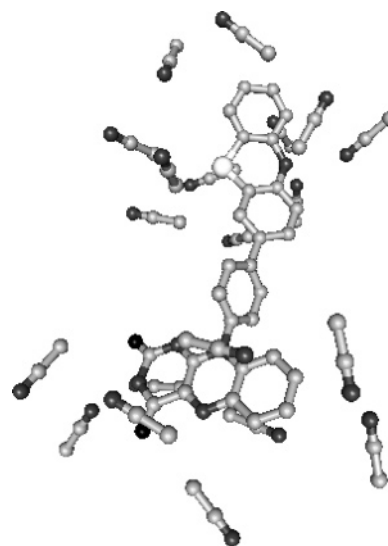
bond distance	loc.	S <sub>0</sub>	LE-min ( $\Delta$ )	CI ( $\Delta$ )	CT-min ( $\Delta$ )
C21-N29	iso.	1.294	1.362 (6.8)	1.341 (4.7)	1.380 (8.6)
N26-C27	iso.	1.381	1.412 (3.1)	1.406 (2.5)	1.418 (3.7)
C22-N35	iso.	1.298	1.327 (2.9)	1.320 (2.2)	1.332 (3.4)
C36-O37	iso.	1.210	1.235 (2.5)	1.230 (2.0)	1.239 (2.9)
C21-C22	iso.	1.469	1.436 (-3.3)	1.445 (-2.4)	1.428 (-4.1)
C21-C27	iso.	1.505	1.472 (-3.3)	1.481 (-2.4)	1.464 (-4.1)
C 3-N31	pht.	1.399	1.378 (-2.1)	1.383 (-1.6)	1.368 (-3.1)
C 4-S 8	pht.	1.784	1.756 (-2.8)	1.763 (-2.1)	1.742 (-4.2)

<sup>a</sup> For the numbering of the atoms, see Figure 1.

minimum, and the same applies also to the bond lengths compiled in Table 4.

**At the LE Minimum-Energy Geometry.** The LE minimum-energy geometry does not lie within  $\mathcal{V}$  since the nuclear degrees of freedom in the orthogonal complement to  $\mathcal{V}$  are relaxed for the CT and not the LE state. Hence, the actual LE minimum lies energetically a bit below its projection onto the  $\mathcal{V}$  subspace. Nevertheless, we denote the projection of the LE minimum onto  $\mathcal{V}$  as the “LE minimum” for the following discussion.

Considering Figure 3a, one can conclude that (i) there exists a conical intersection seam in the low-energy region of the CT and LE surfaces, (ii) the downhill path from the Franck–Condon (FC) point on the LE surface to the LE minimum does not lead directly through the conical intersection seam, and (iii) the LE minimum and the CT minimum are separated by a comparatively low barrier of less than 1 kcal/mol, perhaps somewhat larger taking into account that we only consider the LE minimum projected onto the  $\mathcal{V}$  subspace. Hence, the question regarding to what extent the CI seam is responsible for fast transfer of the population from the bright LE state to the dark CT state cannot conclusively be answered from this picture. However, one has to realize that this is the situation in the gas phase, while all experimental measurements, so far, have been performed in solution. It is anticipated that solvent effects dramatically stabilize the CT state (due to its large dipole moment) relative to the LE state, primarily due to dipole–dipole interactions for polar molecules but also due to inductive interactions in less polar solvent environments. As a result, the conical intersection seam is expected to be shifted in position toward the FC point on the LE surface. Since the two surfaces are quite close already at the FC point, a relevant question to be answered is if the CT surface now moves below the LE surface at the GS minimum structure due to solvent effects, such that the CI seam now is above the FC point, becoming irrelevant for the subsequent photophysical processes. In order to describe solvation effects, computationally rather inexpensive continuum model approaches are frequently employed. However, the results from continuum model calculations may sensitively depend on the specification of the molecular cavities,

**Figure 4.** Solvent cluster consisting of the dyad (solute) and 20 acetonitrile (solvent) molecules.

that is, the radii of the spheres used for their construction. In particular, spheres used for atoms in ions or zwitterions should be specified differently from those of atoms in neutral molecules.<sup>88</sup> In order to avoid any arbitrariness caused by different specifications of such spheres for the LE and CT states, we instead performed calculations for a solvent cluster including the dyad solute surrounded by 20 acetonitrile solvent molecules. Such an approach is, of course, much more expensive and became only feasible recently by virtue of recent advances in local correlation methods.<sup>81</sup>

**Solvent Effects.** Local CC2 excitation energies for the LE and the CT states were calculated for the dyad in the GS minimum geometry within a cluster of 20 acetonitrile solvent molecules. The geometry of the solvent cluster was generated according to the following three steps. (i) The dyad plus eight nearest acetonitrile molecules were optimized at the DFT level in order to relax the dyad in the presence of a few solvated molecules. (ii) The dyad structure so obtained was solvated with 480 acetonitrile molecules, and the structure and positions of these solvent molecules were then optimized by using the classical force field implemented in the MOLOC program.<sup>89,90</sup> The structure of the dyad solute molecule was kept frozen in this process. (iii) All solvent molecules within a radius of 9 Å from the midpoints of each chromophore (i.e., the midpoints of the middle rings in isoalloxazine and phenothiazine) were selected and included in the subsequent local CC2 calculations. The resulting solvent cluster shown in Figure 4 comprises 20 acetonitrile solvent molecules. This cluster, of course, reflects just one particular low-energy configuration of the heterogeneous solvent environment. However, in order to answer our rather qualitative question about the order of the two states in the presence of a solvent environment, we think that this is a viable approach. The corresponding local CC2 calculations are still rather expensive and belong, to our knowledge, to the largest excited-state calculations performed so far at a level beyond TD-DFT.

(88) Barone, V.; Cossi, M.; Tomasi, J. *J. Chem. Phys.* **1997**, *107*, 3210.

(89) Gerber, P. R. *J. Comput.-Aided Mol. Des.* **1998**, *12*, 37.

(90) Gerber, P. R.; Müller, K. *J. Comput.-Aided Mol. Des.* **1995**, *9*, 251.

(91) Boughton, J. W.; Pulay, P. *J. Comput. Chem.* **1993**, *14*, 736.

**Table 5.** Excitation Energies (eV), Oscillator Strengths (Length Representation), and Excited-State Dipole Moments (debye) for the Dyad and the Dyad Solvent Cluster (Dyad Plus 20 Acetonitrile Molecules)<sup>a</sup>

structure	state	TD-DFT/B3-LYP			LCC2
		E(eV)	f	$ \bar{\mu}(\text{ex}) $	E(eV)
dyad	LE	3.029	0.189	13.018	<b>3.160</b>
dyad+20 ACN	LE	2.807	0.1715	28.11	<b>2.798</b>
dyad	CT	1.834	0.002	46.034	<b>3.550</b>
dyad+20 ACN	CT	1.753	0.0068	54.52	<b>3.120</b>
$\Delta$ LE		-0.222			-0.362
$\Delta$ CT		-0.081			-0.430
$\Delta$ CT- $\Delta$ LE		0.141			<b>-0.068</b>

<sup>a</sup> For the local CC2 calculation, only the excitation energies are given.  $\Delta$ LE and  $\Delta$ CT are the solvatochromic shifts (eV) obtained as the differences of the excitation energies in the gas phase and the solvent cluster environment.

The TD-DFT and LCC2 results obtained for this solvent cluster are compiled in Table 5. It is noteworthy that the CIS method is not able to find an excited state with dominant charge-transfer character. Our calculations show that none of the states with a reasonable HOMO–LUMO singles contribution (essential for considering the corresponding excited state as the CT state) in their excitation vector exhibit a sufficiently large excited-state dipole moment. This holds true for the isolated dyad, as well as for the dyad solvent cluster. Nevertheless, the domains provided by the CIS wave function for the subsequent LCC2 treatment are sufficient to pick up and properly describe the CT state (this was already found to be the case in ref 81). As can be seen from Table 5, the solvent environment shifts the excitation energy of the LE state from 3.160 to 2.798 eV. A further shift of 0.13 eV to the red is observed on going from the cc-pVDZ to the bigger aug-cc-pVDZ basis (isolated dyad). Taking this into account, we end up at an excitation energy of 2.67 eV for the LE  $\leftarrow$  S<sub>0</sub> excitation in the solvent cluster, which is not too far from the red onset of the LE absorption band at 2.53 eV measured by Schneider et al.<sup>28</sup> The omission of the side chain and methyl group has only a minor effect on the excitation energies, as already shown before.<sup>81</sup> The excitation energy for the CT state, on the other hand, is shifted from 3.550 to 3.120 eV, leading to a net stabilization of the CT state relative to the LE state of 0.068 eV, which is far from the value required to switch the order of the states at this geometry (note that we have taken the most polar solvent used in the experiment). Nevertheless, already a constant shift of the CT surface relative to the LE surface by -0.068 eV is sufficient to remove the original barrier between the LE and CT minima entirely, such that the CI seam now comes into play, as shown in Figure 3b. One can further anticipate that, close to the CT minimum, where the solvent molecules are allowed to reorient according to the bigger dipole of the CT state, the stabilization of the CT relative to the LE state is much higher than this constant offset of 0.068

eV. Therefore, the CI seam moves much closer to the FC point than Figure 3b is suggesting. We can conclude from our LCC2 calculations on the solvent cluster that (i) the CI seam remains in the low-energy area of the LE and CT surfaces, particularly below the FC point, and hence plays an important role in transferring population from the bright LE to the dark CT state and (ii) the solvent environment plays an important role for the efficiency of the population transfer via the conical intersection.

It is worth mentioning that the TD-DFT calculations, on the other hand, predict a relative stabilization of the LE state relative to the CT state by 0.141 eV (even though the dipole moment of the CT state is even larger than that predicted by CC2), quite the opposite to the LCC2 calculations and also quite contrary to what one would expect from physics. This again illustrates the problems TD-DFT has in describing CT situations.

## Conclusions

In this work, the photophysics of the phenothiazine–phenyl–isoalloxazine dyad synthesized and characterized recently by Daub and co-workers were investigated by using a combination of TD-DFT and coupled-cluster response theory (CC2 model). We have located a conical intersection seam in the low-energy region of the potential energy surfaces of a bright locally excited (LE) and a dark charge-transfer (CT) state. Whether this conical intersection seam leads to fast transfer of the population from the excited LE to the dark CT state remains inconclusive for the molecule in the gas phase. However, for the solvated dyad, the CT state is expected to be strongly stabilized by the solvent environment relative to the LE state with a much smaller dipole moment. In order to show that the solvent environment is not yet shifting the conical intersection seam outside of the low-energy region, that is, above the FC point, we performed local CC2 calculations on a solvent cluster involving the dyad plus 20 additional acetonitrile molecules. On the basis of these calculations, we propose that, for the solvated dyad, fast population transfer indeed occurs from the bright LE to the dark CT state via the conical intersection seam, which hence, is responsible for the observed fast fluorescence quenching and low quantum yield observed in the experiments.

**Acknowledgment.** We would like to thank Dr. M. Bocola for his help concerning the molecular mechanics calculations and Dr. F. Furche, Prof. J. Daub, and Prof. A. Penzkofer for useful discussions. This project is part of the Graduate College Sensory Photoreceptors in Natural and Artificial Systems (GRK 640) in Regensburg, funded by the Deutsche Forschungsgemeinschaft (DFG).

**Supporting Information Available:** Complete ref 83. This material is available free of charge via the Internet at <http://pubs.acs.org>.

JA068536T